THE EFFECT OF START-UP ON FAT (AND WAX) FOULING TESTS

J.-Y. Huang[1], Y.M.J. Chew[2] and D.I. Wilson[1,*]

[1] Department of Chemical Engineering and Biotechnology, University of Cambridge, New Museums Site, Pembroke Street, Cambridge CB2 3RA, UK.
[2] Department of Chemical Engineering, University of Bath, Claverton Down, Bath, BA2 7AY, UK.

*E-mail: diw11@cam.ac.uk

ABSTRACT

The influence of starting mode on the formation of fouling deposits by crystallisation on a cooled surface was studied using binary solutions of tripalmitin in paraffin using a spinning disc system. Studies of the thermal and rheological characteristics of the solutions and gels formed by cooling indicated that low concentrations yielded weak gels which were less able to withstand the shear stresses imposed in the fouling tests. Particulate gels are formed rapidly when the surface temperature exceeds the cloud point. The onset of deposition, like the cloud point, is sensitive to cooling rate and shear stress. Initial fouling behaviour is therefore very sensitive to the start-up protocol. Subsequent deposition exhibited a constant fouling rate, followed by falling rate behaviour, for concentrations giving strong gels. Solutions with low concentration of tripalmitin give sigmoidal fouling resistance plots, indicating shear induced removal in the early stages of fouling. The constant and falling rate regime parameters were not affected by the start-up mode. Deposit sloughing was observed at high surface supercooling.

INTRODUCTION

Mixtures of food fats can cause severe deposition on cold surfaces as these materials exhibit normal solubility behaviour and are less soluble at low temperature. Fouling in food fats shares many similarities with wax deposition from crude oils in undersea pipelines, but has received less attention because the flow channels are significantly shorter and easier to maintain. Similarities include the multi-component nature of the solutions, *i.e.* there are many species present which could solidify, and the high cost of a plugging incident. Differences include the high concentration of solidifying species in food fat mixtures and the product quality aspect: the extent of crystallisation in a food fat mixture (*e.g.* a filling) is an important product characteristic for subsequent processing steps and fouling can cause loss of temperature control and variation in mixture characteristics.

A particular feature of fat and wax fouling is the build-up of gels on the cold surface, in addition to surface-induced growth. This is promoted by the formation of non-spherical crystals which give rise to yield stress-behaviour at relatively low volume fractions (De Graef *et al*., 2008). When the gel 'strength' is large enough to withstand the shear stresses imposed by the liquid flow, the material forms a static (fouling) layer at the wall. The material can subsequently undergo ageing, modifying its rheological characteristics. Wax fouling in crude oil pipelines driven by gel formation and ageing has been studied extensively by Fogler and co-workers (*e.g.* Singh *et al.* (2000), Venkatesan *et al*. (2005), Lee *et al*. (2008)). Thermal aspects are still important, as the temperature field determines the onset of crystallisation and gel formation: workers such as Bidmus and Mehotra (2004) state that heat transfer aspects dominate.

Several experimental techniques have been used to study fouling from wax and fat solutions, such as flow loop and cold-finger devices. The importance of controlling temperature and shear stress conditions at the test surface prompted Nigo *et al.* (2009) to develop a novel spinning disc apparatus (SDA) featuring a cooled rotating stainless steel plate as the test section. The spinning disc configuration provides uniform rates of heat and mass transfer (but varying shear stress) across the surface, and its operation can be simulated readily by computational fluid dynamics (CFD). Nigo *et al.* investigated deposition from model binary solutions of tripalmitin (PPP, a high melting point triglyceride present in palm oil) in paraffin which had been studied previously by Fitzgerald *et al*. (2004) using a channel flow test section.

Nigo *et al.* reported fouling in terms of deposit mass. Huang *et al*. (2012) extended the SDA capability by monitoring deposition on-line via thermal measurements using a heat flux sensor mounted behind the test surface. They reported three stages of fouling: (*i*) an initial, rapid

step in fouling resistance, R_f, associated with gel formation when the cold surface was initially contacted with warm solution; (ii) a period of linear fouling (dR_f/dt constant, where t is time), which terminated when the estimated deposit surface temperature reached a critical value, labelled T^*, and (iii) falling rate fouling (dR_f/dt decreased with time) and asymptotic behaviour as the surface temperature approached the solid/liquid equilibrium temperature of the solution. The growth rate in stage (iii) followed normal growth kinetics (Borisov et al., 1968). The R_f-t profiles were qualitatively similar to Kern-Seaton (1957) behaviour but did not give good quantitative agreement with their model.

This paper extends the earlier work by Huang et al. to investigate the effect of concentration of crystallising species (PPP) on deposition, and to determine the effect of experimental start up on the observed fouling behaviour. Furthermore, the SDA heat flux sensor was replaced by one containing an integral thermocouple, allowing more accurate estimation of the surface (metal and deposit-liquid) temperature. This facility, combined with accurate CFD simulations, allowed the surface temperature and shear stress to be manipulated independently by adjusting the rotation speed ω_d and the coolant temperature, T_{cw}: this is not readily achieved in flow loop and cold-finger systems.

The starting mode is an important consideration in fat and wax testing as there can be no induction period as gel formation is not necessarily driven by surface growth. The initial rate of fouling can be fast and is sensitive to the initial conditions. Gels can form rapidly when the solution is subcooled, and crystallisation initiated by homogeneous nucleation (quantified as the solution cloud point, T_c) is a random process influenced by the local cooling rate (Mullin, 1993). Deposit formation can be driven by a number of scenarios, including changes in solution temperature, wall temperature, solution concentration, and flow stoppage. It is important that variations in behaviour arising from different initiation conditions are understood so that appropriate operating modes and process models can be developed.

Four starting modes were tested under notionally identical conditions, illustrated in Figure 1: (a) 'cold start', used by Huang et al. (2012): the test surface, T_s, is initially at the coolant temperature, T_{cw}, which is lower than the set point temperature for steady state heat transfer, T_{set}, and increases when the surface is immersed in the test solution (at temperature T_b): (b) 'warm start', with the test surface notionally starting at T_{set}; (c) 'cooling start', test surface initially at bulk solution temperature, T_b, and cooled to the desired surface temperature, T_{set}; and (d) 'chemical start', where fouling is started by injecting concentrated PPP solution into the bulk liquid: thermal steady state has been established previously with a charge of paraffin in the SDA reservoir. A detailed description of the tests is given in Huang et al. (2013): this paper summarises that work and highlights certain aspects for note by fouling researchers.

MATERIALS AND METHODS

A detailed description of the SDA and its operation is given in Huang et al. (2012) and Huang et al. (2013).
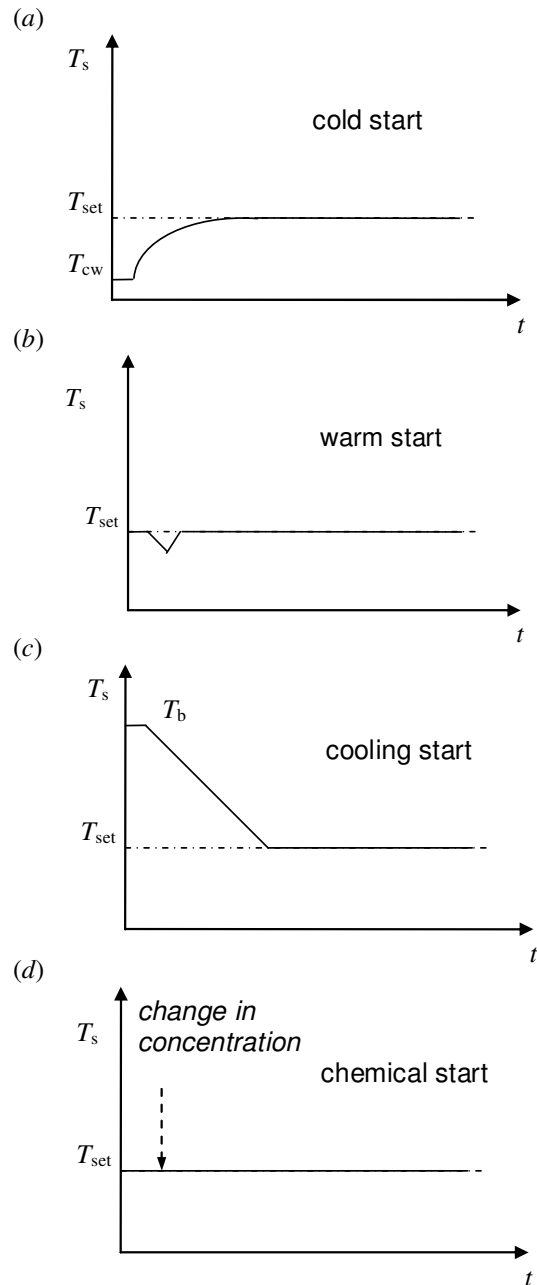

Fig. 1. Schematics of evolution of test surface temperature, T_s, under different start-up modes. (a) 'cold start'; (b) 'warm start'; (c) 'cooling start'; (d) 'chemical start'. Dashed horizontal line indicates target value, T_{set}.

In brief, it consists of a rotating stainless steel can of diameter 8 cm with well-insulated sides so that heat transfer occurs mainly through the base. The base consists of a brass block in which a heat flux sensor (Rhopoint, UK, type 20457-3) with an integral thermocouple is located. Fitted over this is a 4.5 mm thick, removable stainless steel disc which comprises the test surface. The material and morphology of the test surface can be modified as desired.

The temperature of the test surface is determined by the rotation speed (provided by a stepper motor), the bulk solution temperature and the temperature of a water-based

coolant liquid which is recirculated through the can by a separate thermostat. The temperature at the heat flux sensor and the heat flux across the sensor are monitored by solid-state data collection devices attached to the can. Data from these are transferred to a PC at the end of an experiment.

Normally 2 L solution was held in an insulated cylindrical vessel and maintained at bulk temperature T_b by circulation of hot water through its heating jacket. The solution was stirred by a magnetic stirrer.

Model fat solutions were prepared by dissolving tripalmitin (PPP, > 85% purity; Sigma Chemicals, UK) in paraffin oil (density at 25 °C, 870 kg m^{-3}; BDH Chemicals, UK) at 60 °C. This temperature is employed to eradicate thermal history of crystallization, as it promotes dissolution of any small crystals present in solution which may otherwise facilitate heterogeneous nucleation (see Fitzgerald *et al.*, 2004). The concentrations of the model solution used in this study are summarised in Table 1. Melting points were determined using differential scanning calorimetry (scanning at 10 K/min) and cloud points by turbidity measurements (at a cooling rate of 0.5 K/min). Details of the protocols are given in Huang (2012).

Table 1 Measured transition temperatures for PPP solutions

Concentration (wt%)	2.5	3.75	5	10
Melting point, T_m (°C)	46.6	48.4	49.1	51.8
Cloud point, T_c (°C)	24.9	28.4	29.8	38.4

The process of gelation in the presence of shear in the test solutions was investigated separately using the technique employed by De Graef *et al.* (2008) and Tarabukina *et al.* (2009). A sample of solution was located in the gap between two parallel plate tools of a Bohlin CVO 120 controlled-stress rheometer and heated to ~60°C (the bulk temperature in SDA fouling tests). The shear stress imposed on the sample was maintained constant 2 Pa, while the temperature was reduced at a rate of 5 K/min to a target value, and held there. It should be noted that the shear stress varies with radial position when parallel plate tools are used: the value quoted is that at the plate rim. The instantaneous apparent viscosity data are presented as the relative viscosity of the solution, *i.e.* divided by the viscosity of the Newtonian paraffin solvent at the same temperature.

The 2 Pa shear stress setting employed is typical of the values generated at the edge of the disc in the SDA device, calculated from CFD simulations (see Huang, 2012), and is therefore representative of the shear stress exerted by the solution on the clean metal surface and deposit-solution interface during fouling tests.

All SDA tests were performed with T_b = 60°C. In *cold start* experiments, coolant was circulated through the can so that its temperature reached T_{cw} before it was immersed in the solution, which had been preheated to T_b. Separate heat transfer tests (an example is shown in Figure 4(*b*)) with

paraffin alone indicated that the thermal transient associated with this start mode lasted around 3 min. In *warm start* experiments, the SDA can was immersed in a small bath of paraffin at 60°C, rotated and coolant circulated until thermal steady state was reached. Rotation was stopped momentarily and the can transferred to the test solution vessel and the experiment started. In *cooling start* experiments, the can temperature was gradually lowered by circulation of the coolant. The time at which deposition was evident in the R_f-t profiles was denoted t_{on}, and often occurred before T_{cw} reached its target temperature. In *chemical start* experiments, a charge of 200 mL of concentrated PPP solution was injected into the bulk liquid above the stirrer when thermal steady state had been reached. Dye tracer experiments established that thorough mixing of the solution took 2-3 minutes.

On completion of a test the deposit was photographed, weighed, then removed from the plate and analysed for solids content (by filtration), total PPP concentration (by gas chromatography) and estimated PPP concentration in the interstitial voids (by difference). The latter quantity was subject to systematic errors and sometimes gave erroneous results. The deposit layers after a 12 h test were uniformly distributed (except where spalling occurred) particulate gels, with thickness of about 1-3 mm.

Fouling was monitored by the change in overall heat transfer coefficient, U, calculated from the measured heat flux, q, via

$$R_f(t) = \frac{1}{U(t)} - \frac{1}{U(0)} = (T_b - T_{cw})\left\{\frac{1}{q(t)} - \frac{1}{q(0)}\right\} \quad (1)$$

This expression assumes that the film heat transfer coefficient for convection in the solution is constant. In practice this changes owing to the reduction in viscosity in the thermal boundary layer as the deposit/solution interface temperature increases. Separate heat transfer studies allowed the R_f values to be corrected for this effect. Figure 2 shows that this correction is small and does not alter the trend. The three stages in fouling described above are again evident.

RESULTS AND DISCUSSION
Gelation Behaviour
The formation of a gel as the solutions are cooled while being sheared is accompanied by a sharp increase in the relative viscosity, marked as the boundary between regions A and B on Figure 3. This occurs at lower temperatures for lower concentrations, as the cloud point (Table 1) is lower.

The 5 wt% and 10 wt% data sets quickly reach relative viscosities of 10,000 and the increase thereafter (marked B-C is more gradual (on a log scale) as the crystal network spanning the rheometer gap is established. After some time the trend is noisy, which is related to slip on the plates and local fracture of the gel, *i.e.* soft solid behaviour. Similar features were reported for palm oil by Tarabukina *et al.* (2009). The large fluctuations in the plateau region (marked D) are associated with stick and slip on the rheometer plates.
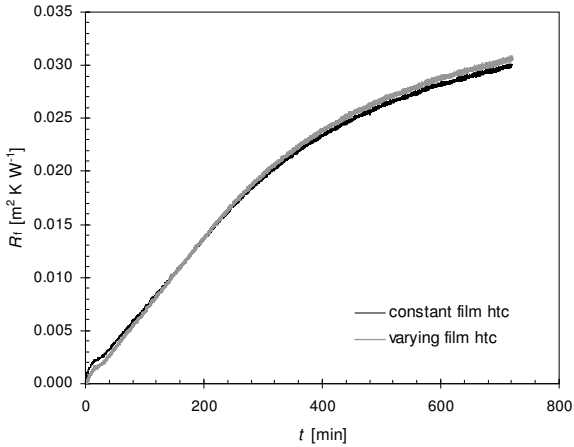
Fig. 2 Evolution of fouling resistance with time for 5 wt% PPP solution, T_b = 60°C, T_{cw} = 9.8 °C, warm start mode, ω_d = 5.4 rad/s. Loci show the effect of recalculating solution film heat transfer coefficient based on T_s.

The Figure shows that the 5 and 10 wt% solutions will form plastic masses which can withstand shear stresses of 2 Pa readily. In contrast, the 2.5 wt% solution does not give a sharp increase and exhibits a plateau around relative viscosity ~ 10, indicating that this solution does not form a strong gel under these conditions.
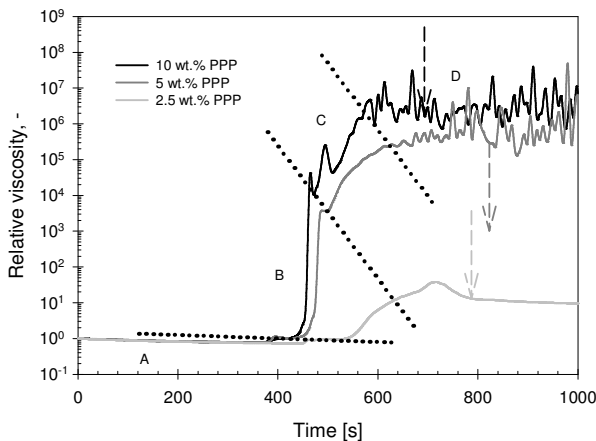

Fig. 3. Evolution of relative viscosity for PPP solutions undergoing cooling at 5 K/min under a steady shear stress of 2 Pa. Dashed lines indicate different regimes. Vertical arrows show the end of the cooling stage: 60 − 10 °C for 10 wt.% PPP, 55 − 5 °C for 2.5 and 5 wt.% PPP solutions. Reproduced from Huang *et al.* (2013).

Cold Start vs Warm Start

Figure 4 shows the results obtained for notionally identical experiments performed under cold start and warm start mode which was intended to eliminate the initial heat transfer transient. The fouling profiles are very similar over the 12 h test, with a small difference in the initial step in R_f which increases gradually over time. The linear fouling rate is slightly different but the temperature at the transition to the falling rate stage, T^*, was similar (within experimental error) and the kinetic constant in the latter stage was also similar. The detailed record of the initial transient in Figure

4(*b*) shows negative R_f values, even in paraffin, confirming that these are artefacts resulting from immersing the cold test plate in the warm test solution, momentarily increasing q in Equation (1) above the steady state value. Whereas the paraffin reaches a steady, non-fouled stage after 3 min, by this time there is an appreciable gel layer (R_f ~ 1 m^2 K/kW) in the cold start case. The warm start profile shows a gradual increase after the initial dip, and a smaller increase in R_f is evident after 5 min.
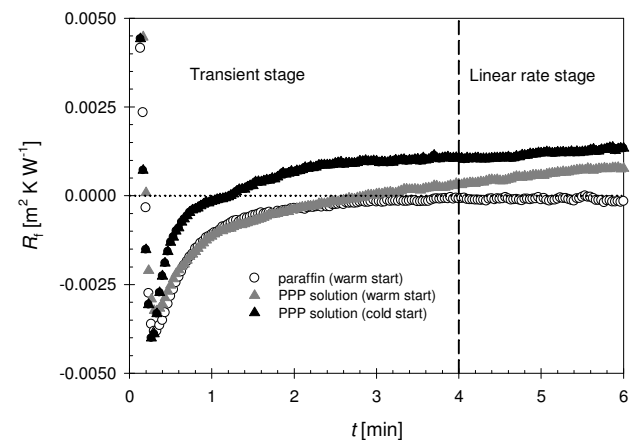
(*a*)
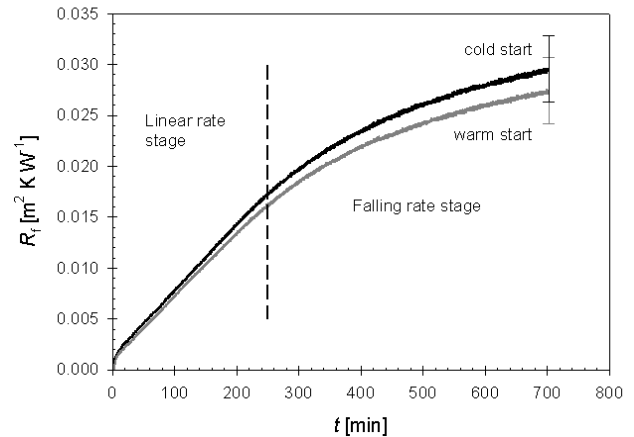
(*b*)

Fig. 4 Comparison of cold and warm starting modes for 5 wt% PPP solutions at T_b = 60 °C, T_{cw} = 9.8 °C, ω_d = 5.4 rad/s. (*a*) 12 h test - vertical dashed line separates the linear rate stage from the falling rate stage. Error bars refer to uncertainty in the R_f estimates. (*b*) Initial stage, including data from heat transfer tests using paraffin alone. Reproduced from Huang *et al.* (2013).

Warm start mode was also reproducible, and was employed in studies of the effect of coolant temperature (see Huang *et al.*, 2013) and wall shear stress. Reproducibility was determined by conducting a series of experiments under identical conditions for various times. The R_f-t plots showed good agreement, with a maximum difference of 3% and 5%, respectively.

Figure 5 shows the R_f-t profiles obtained for 5 wt% solutions subjected to initial wall shear stresses of 0.26-1.66

Pa, at an initial surface temperature of 21.8 °C. This was achieved by manipulating the coolant temperature in CFD calculations and confirmed by separate heat transfer tests. Figure 5(a) shows small differences in the initial step in R_f, followed by linear fouling at very similar rates (no statistically significant difference). The temperature of the transition to the falling rate regime, T^*, was also similar, at 34.1 – 35.3 °C. The R_f-t profiles in the falling rate regime diverge noticeably. This is due to the deposit-solution film heat transfer coefficient depending on rotation speed. The deposit-solution interface temperature (and the fouling rate) is therefore also sensitive to rotation speed.
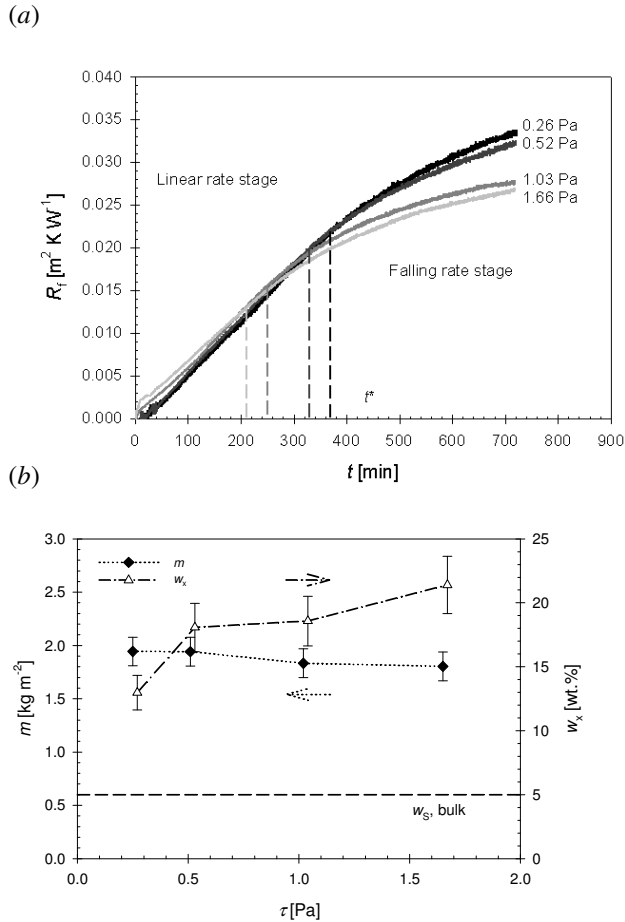
(a)

(b)

Fig. 5 Effect of initial average wall shear stress on the (a) R_f-t profiles and (b) final mass and composition of deposits. Conditions: 5 wt.% PPP solution, $T_b = 60$ °C, $T_{cw} = 9.8$ °C, warm start mode. Reproduced from Huang *et al.* (2013). The horizontal dashed line indicates the initial concentration of PPP in the bulk solution.

The insensitivity of the linear fouling rate (around 10^{-6} m^2 K/J) to the imposed shear stress indicates that the mechanism is not controlled solely by heat, mass or momentum transport. Furthermore, the T^* value (~35°C for 5 wt% solutions) lies within the metastable region for crystallisation, *i.e.* $T_c < T^* < T_m$ so is not associated with these limiting phenomena.

Previous investigations by Nigo *et al.* (2009) on similar solutions included electron microscopy and X-ray diffraction analysis of the deposits at different stages. There was no noticeable change in crystal polymorph or shape over the course of the fouling runs, indicating that a chemical transition was not the source of the change in fouling behaviour.

Tests stopped after 1, 3, 6 and 9 h showed an increase in the deposit solids level with time, indicating that the gels undergo rapid ageing. The composition of the final deposits in Figure 5(b) show that the gels formed were considerably richer in PPP than the bulk solution. Furthermore, the deposit solids content, w_x, was larger in those gels formed under higher shear stresses, suggesting that the gel microstructure and rheology was determined by the conditions prevailing at its formation. This is analogous to biofouling, where dense, strong biofilms are formed when the bulk liquid velocity is high (Bott, 1995). The link between gel microstructure, rheology, heat transfer and history require further elucidation but are important for understanding processes in oil pipelines (*e.g.* Marchesini *et al.,* 2012).

Cooling Start

Figure 6 shows that it took over an hour for the coolant to reach its target temperature (at time t_t). This mode did, however, eliminate the transient in R_f arising from changes in U at the time when deposition starts (*e.g.* Fig. 4(b)). Fouling starts at t_{on}, and here and in most other cases studied, $t_{on} < t_t$. The log scale obscures the fouling behaviour, which was similar to those reported above, with a small initial step in R_f and similar linear fouling rates.
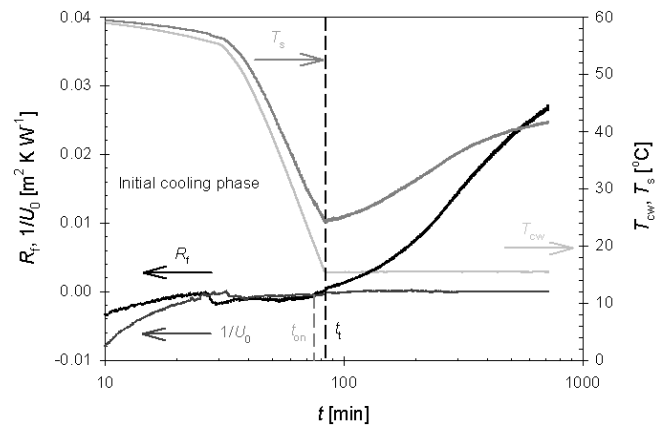

Fig. 6 Evolution of R_f, T_s and T_{cw} for 5 wt.% PPP solution tests in cooling start mode. $T_b = 60$ °C, $T_{target} = 14.8$ °C, $\omega_d = 5.4$ rad/s. $1/U_0$ data from paraffin heat transfer test. Note log scale on time axis. Vertical lines indicate when fouling is detected, t_{on}, and when T_{cw} reached its setpoint, t_t. Reproduced from Huang *et al.* (2013).

Also plotted in Figure 6 is the substrate (the deposit)-solution interface temperature, T_s. It can be seen to fall to a value close to the cloud point (Table 1) before fouling starts, but increases beyond the cloud point as the deposit grows. This suggests that initial gel formation is related to

homogeneous precipitation but subsequent growth occurs via a heterogeneous mechanism promoted by the existing crystal network.

Table 2 is a summary of an investigation of T_{target} on fouling behaviour. The R_f-t profiles were similar to Figure 6 with the exception of that at the lowest T_{target} (highest subcooling), which exhibited deposit spalling and sawtooth behaviour. As T_{target} decreased, the estimated temperature at which deposition started, $T_{s,on}$, also decreased and in all cases was lower that the cloud point. The initial step increase in R_f varied with T_{target} (and subcooling at the point of gel formation, driving solidification) but the subsequent linear fouling rates were similar, except where spalling was observed. The falling rate kinetics were also similar (data not reported). These results highlight how the onset of gel formation is a kinetic process and cannot be described by a single parameter associated with a single mechanistic step.

Table 2 Effect of extent of cooling on fouling behaviour. 5 wt.% PPP solution, T_c = 29.8 °C, ω_d = 5.4 rad/s

| T_{target} (°C)	$t_t - t_{on}$ (min)	$T_{s, on}$ (°C)	Linear fouling rate (10^{-6} m^2 K/J)
14.8	20.0	23.2	1.17
9.8	20.0	22.1	1.25
7.3	12.3	21.2	1.11
4.8	8.5	20.6	0.57*

* deposit spalling occurred

The cooling start mode was used in a brief investigation of the effect of solution concentration, summarised in Figure 7. The coolant temperature was selected to be 20 K below the solution cloud point in each case. The R_f-t profiles exhibit similar behaviour for the 3.75, 5 and 10 wt% solutions, whereas the 2.5 wt% solution exhibits sigmoidal behaviour. The linear fouling rates obtained for the three higher concentrations were roughly proportional to the bulk concentration. This aspect is not yet fully understood.

The sigmoidal behaviour observed at the lowest concentration is consistent with the rheology results in Figure 2, which indicated that the gel formed by the 2.5 wt% solution would be susceptible to deformation by an imposed shear stress of 2 Pa. The cooling start mode also involves a smaller amount of surface supercooling ($T_m - T_s$) than the cold and warm start modes, reducing the thermodynamic driving force for initial precipitation and therefore solids content and yield strength of the initial gel formed at the heat transfer surface. Estimates of the deposit-solution interface temperature and shear stress applied to the interface by the liquid indicated that it started to grow in a linear fashion once the stress imposed by the liquid fell below 2 Pa. This sigmoidal behaviour was also observed in 'chemical start' tests on 2.5 wt % solutions (see Fig. 8), whereas 5 wt% solutions exhibited a nearly linear-falling rate behaviour, as observed with other start modes.

The deposit mass and composition results in Figure 7(b) show an increase in final mass with PPP concentration, which is consistent with the final R_f values in Figure 7(a). The thermal conductivity of the fat crystals is similar to the solution, and plots of R_f against final mass for all the tests here exhibited a linear relationship confirming this. The solids mass fraction, w_x, however, increases strongly with PPP concentration, indicating the formation of strong gels by rapid ageing. The concentration of PPP in the solution trapped in the gel, w_s, also increases with bulk concentration and at higher concentrations appears to be larger than the bulk concentration. The latter is considered an unphysical result: the error bars for these data are large and the values are very sensitive to the value of w_x. A more accurate method for determining w_x, such as quantitative NMR, is under consideration.
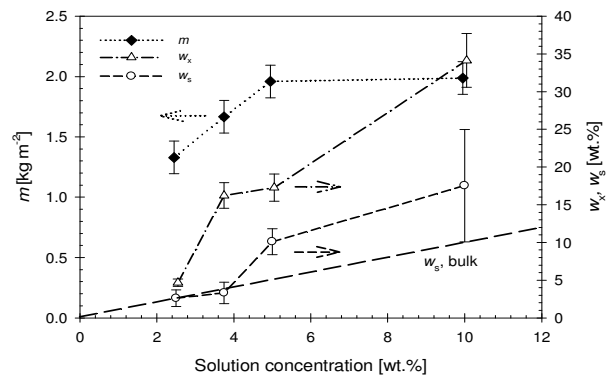
(a)
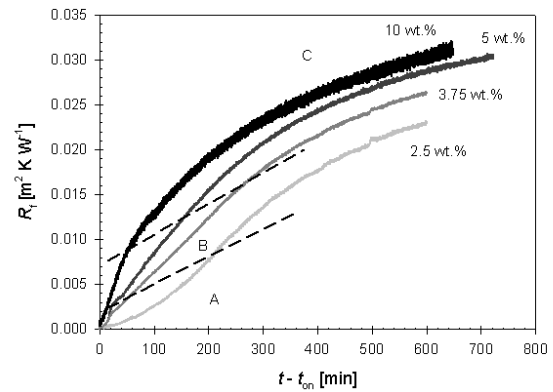
(b)

Fig. 7 Effect of solution concentration on (a) fouling behaviour and (b) deposit composition at end of test. T_b = 60°C, ($T_c - T_{cw}$) = 20 K, ω_d = 5.4 rad/s. AB boundary separates initial and linear fouling rate stages; BC separates linear and falling rate behaviours. Time ordinate is time elapsed since deposition started. Figure (a) reproduced from Huang *et al.* (2013).

Figure 7(b) nevertheless confirms that the deposit solids content, and hence microstructure and response to shear stress, is strongly affected by the concentration of solidifying species in solution. These tests have only considered binary solutions of one crystallising species in

solution: the presence of further crystallising species, mimicking real solutions, has yet to be investigated.

Chemical Start

In this mode, fouling is induced by introduction of concentrated PPP solution. Trial runs using injection of paraffin alone confirmed that the thermal conditions were not interrupted. The R_f–t data for the 5 wt% test in Figure 8 exhibit similar behaviour to the other start modes, except that there is no initial step in R_f associated with initial subcooling-driven nucleation. This aspect is illustrated in Figure 9. Both the cooling and chemical start modes exhibit linear increase in R_f once deposition starts. There is a ramp in the former profile after 15 min which is attributed to the coolant reaching its target temperature. The negative R_f transients for cold and warm start modes are evident.
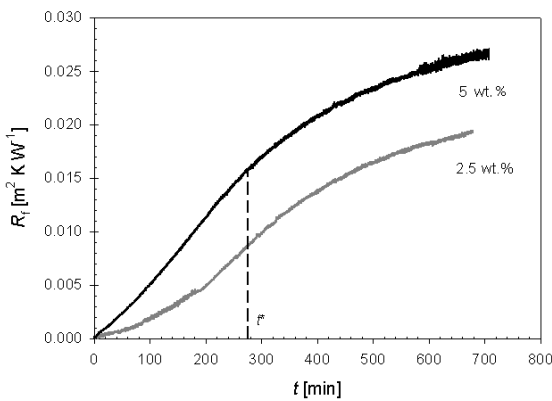

Fig. 8 Effect of solution concentration on fouling behaviour in chemical start mode: $T_b = 60$ °C; $(T_c − T_{cw}) = 20$ K $\omega_d = 5.4$ rad/s. Reproduced from Huang *et al.* (2013).

Figure 9 indicates that the chemical start mode is best for fundamental investigations of this type of fouling. It does, however, require more resources (adding the solute to pure solvent for each test) and is not appropriate for real solutions, unless the crystallising species can be reliably isolated from inert components.
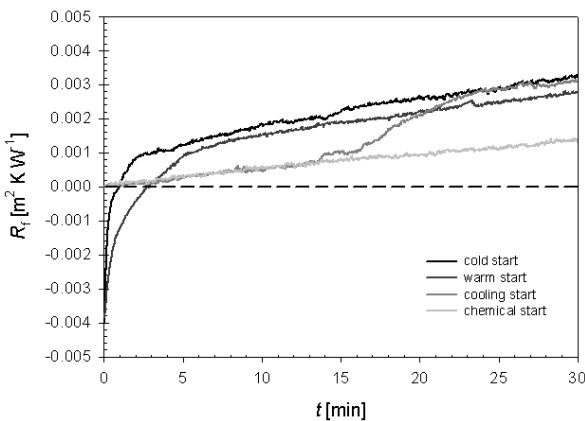

Fig. 9. Effect of starting mode on initial fouling behaviour experiments performed under notionally identical conditions: 5 wt.% solution, $T_b = 60$ °C, $T_{cw} = 9.8$ °C, $\omega_d = 5.4$ rad/s. Time is relative to appearance of first deposit or contact with warm solution. Reproduced from Huang *et al.* (2013).

For cases where chemical start mode cannot be employed, it is desirable to know how the start mode can influence the results obtained. Table 3 summarises the key parameters extracted from the 12 h long tests related to Figure 9. The growth constant K is obtained by fitting the data in the falling rate stage to the normal growth equation

$$G \equiv \frac{d\delta}{dt} = \lambda_f \frac{dR_f}{dt} \equiv K(T_m − T_s) \qquad (2)$$

where δ is the estimated deposit thickness and λ_f its thermal conductivity (taken to be 0.15 W/m K; Huang, 2012).

The initial cooling rates in the four start modes differ by over two orders of magnitude, but the linear fouling rate, T^* and K values all agree within the range of experimental uncertainty. The final solids composition, w_x, varies significantly but this is expected as it relates to the deposit's history. Those which have been subjected to higher initial subcooling (cold and warm start) will have started with a higher solids content gel which will age to a greater degree.

Table 3 Effect of starting mode on fouling parameters and deposit composition for 12 h long tests (Figure 9)

Starting mode	Cooling rate	Linear fouling rate	T^* [a]	K	w_X
	(K/min)	(m^2 K/J)	(°C)	(µm/s K)	(wt%)
Cold start	30.8	1.1×10$^{−6}$	36.2	1.3	18.7±2.0
Warm start	11.6	1.1×10$^{−6}$	34.1	1.2	18.6±1.9
Cooling	0.6	1.2×10$^{−6}$	32.9	1.2	17.3±1.8
Chemical	0.2	1.1×10$^{−6}$	32.6	1.1	13.3±1.4

[a] Uncertainty in $T^* \pm 3.5$ K

These results indicate that the steady growth and falling rate regimes are relatively insensitive to the initial conditions once fouling is established, but the initial fouling behaviour is very sensitive to the starting mode.

CONCLUSIONS
1. The influence of starting mode was investigated in detail using the modified spinning disc apparatus.
2. The R_f–t profiles exhibited an initial transient which was dictated by the starting mode, followed by period of linear fouling (constant rate) followed by falling rate and approach to an asymptote. Surface temperature is a key factor. The linear fouling regime was relatively insensitive to shear stress and strongly dependent on solution concentration.

3. Deposits exhibited significant ageing, increasing in solids content over time.

4. Low fat concentrations gave weaker gels which could be removed by shear, giving sigmoidal R_f-t profiles.

5. For real solutions, where the chemical start mode cannot be employed, care needs to be taken in planning and interpreting the initial stages of fouling experiments.

ACKNOWLEDGEMENTS

NOMENCLATURE

Roman

G Deposit thickness growth rate, μm/s
K constant in Eq. 2, μm/s K
m Mass coverage of deposit, kg/m^2
q Heat flux, W/m^2
R_f Fouling resistance, m^2 K/W
t Time, s
t^* Time at the end of linear fouling stage, s
t_{on} Time at which deposition starts, s
t_t Time to reach coolant target temperature, s
T Temperature, K
T^* Temperature at end of linear fouling stage, K
T_b Bulk temperature, K
T_c Cloud point, K
T_m Melting point, K
T_{cw} Coolant temperature, K
T_s Surface temperature, K
$T_{s,on}$ Surface temperature at which deposition started, K
T_{set} Steady state surface temperature, K
T_{target} Target surface temperature, K
U Overall heat transfer coefficient, W/m^2 K
U_0 Paraffin heat transfer coefficient, W/m^2 K
w_x Concentration of solids in gel, wt.%
$w_{s,}$ Concentration of PPP in solution, by mass, wt.%
$w_{s,bulk}$ Concentration of PPP in bulk solution, by mass, wt.%

Greek

λ_f Thermal conductivity of fouling layer, m K/W
ω_d Disc rotation speed, rad/s

Acronyms

CFD   Computational fluid dynamics
NMR   Nuclear magnetic resonance
PPP   Triplamitin
SDA   Spinning disk apparatus

REFERENCES

Bidmus, H.O., Mehrotra, A.K., 2004, Heat-transfer analogy for wax deposition from paraffinic mixtures, Ind. Eng. Chem. Res., Vol. 43(3), pp. 791-803.

Borisov, V.T., Dukhin, A.I., Matveev, Y.E., Nikonova, V.V., Rakhmanova, E.P., 1968, Kinetics of crystallisation and mechanism of crystal growth in metallic systems, J. Crystal Growth, Vol. 3–4, pp. 663-665.

Bott, T.R., 1995, *Fouling of Heat Exchangers*, publ. Elsevier, Amsterdam.

De Graef, V., Goderis, B., Van Puyvelde, P., Foubert, I., Dewettinck, K., 2008, Development of a rheological method to characterize palm oil crystallizing under shear. Eur. J. Lipid Sci. Tech. Vol. 110(6), pp. 521-529.

Fitzgerald, A.M., Barnes, J., Smart, I., Wilson, D.I., 2004, A model experimental study of coring by palm oil fats in distribution lines, Food Bioproducts Proc., Vol. 82(3), pp. 207-212.

Huang, J-Y., Chew, Y.M.J., Wilson, D.I., 2012, A spinning disc study of fouling of cold heat transfer surfaces by gel formation from model food fat solutions, J. Food Eng., Vol. 109, pp. 49-61.

Huang, J.-Y., 2012, Fundamental features of food fat freezing fouling. PhD Dissertation, University of Cambridge, Cambridge, UK.

Huang, J-Y., Chew, Y.M.J., Wilson, D.I, Investigating the effect of starting mode on food fat gel layer formation on cold surfaces, 2013, J. Food Eng., Vol. 119, 454–463.

Kern, D.Q., Seaton, R.E., 1959, A theoretical analysis of thermal surface fouling, British Chem. Eng. Vol. 4(5), pp. 258-262.

Lee, H.S., Singh, P., Thomason, W.H., Fogler, H.S., 2008, Waxy oil gel breaking mechanisms: Adhesive versus cohesive failure, Energy & Fuels, vol. 22(1), pp. 480-487.

Marchesini, F.H. Alicke, A.A., Paulo R de Souza Mendes, P.R. Ziglio, C.M., 2012, Rheological characterization of waxy crude oils: sample preparation, Energy & Fuels, Vol. 26(5), pp. 2566-2577.

Mullin, J.W., 1993, Crystallisation, 3rd ed, Butterworth-Heinemann, London, UK.

Nigo, R.Y., Chew, Y.M.J., Houghton, N.E., Paterson, W.R., Wilson, D.I., 2009, Experimental studies of freezing fouling of model food fat solutions using a novel spinning disc apparatus, Energy & Fuels, Vol. 23, pp. 6131-6145.

Singh, P., Venkatesan, R., Fogler, H.S., Nagarajan, N., 2000, Formation and aging of incipient thin film wax-oil gels, AIChE J, vol. 46(5), pp. 1059-1074.

Tarabukina, E., Jego, F., Haudin, J.M., Navard, P., Peuvrel-Disdier, E., 2009, Effect of shear on the rheology and crystallization of palm oil, J. Food Sci, Vol. 74(8), pp. E405-E416.

Venkatesan, R., Nagarajan, N.R., Paso, K., Yi, Y.B., Sastry, A.M., Fogler, H.S., 2005, The strength of paraffin gels formed under static and flow conditions, Chem. Eng. Sci, Vol. 60(13), pp. 3587-3598.